J Appl Physiol 134: 1364–1375, 2023.
First published April 13, 2023; doi:10.1152/japplphysiol.00702.2022

american physiological society | JOURNAL OF APPLIED PHYSIOLOGY

RESEARCH ARTICLE

Impact of Climate Change on Health and Performance

Elevations in sweat sodium concentration following ischemia-reperfusion injury during passive heat stress

Hayden W. Hess,[1] Tyler B. Baker,[1] Jason M. Keeler,[1] Jessica A. Freemas,[1] Morgan L. Worley,[2] Blair D. Johnson,[1] and Zachary J. Schlader[1]

[1]*Environmental Physiology Laboratory, Department of Kinesiology, Indiana University Bloomington, Bloomington, Indiana, United States and* [2]*Center for Research and Education in Special Environments, Department of Exercise and Nutrition Sciences, University at Buffalo, Buffalo, New York, United States*

Abstract

Renal ischemia-reperfusion (I/R) injury results in damage to the renal tubules and causes impairments in sodium [Na^+] reabsorption. Given the inability to conduct mechanistic renal I/R injury studies in vivo in humans, eccrine sweat glands have been proposed as a surrogate model given the anatomical and physiological similarities. We tested the hypothesis that sweat Na^+ concentration is elevated following I/R injury during passive heat stress. We also tested the hypothesis that I/R injury during heat stress will impair cutaneous microvascular function. Fifteen young healthy adults completed ~160 min of passive heat stress using a water-perfused suit (50°C). At 60 min of whole body heating, one upper arm was occluded for 20 min followed by a 20-min reperfusion. Sweat was collected from each forearm via an absorbent patch pre- and post-I/R. Following the 20-min reperfusion, cutaneous microvascular function was measured via local heating protocol. Cutaneous vascular conductance (CVC) was calculated as red blood cell flux/mean arterial pressure and normalized to CVC during local heating to 44°C. Na^+ concentration was log-transformed and data were reported as a mean change from pre-I/R (95% confidence interval). Changes in sweat sodium concentration from pre-I/R differed between arms post-I/R (experimental arm: +0.97 [+0.67 − 1.27] [LOG] Na^+; control arm: +0.68 [+0.38 − 0.99] [LOG] Na^+; $P < 0.01$). However, CVC during the local heating was not different between the experimental ($80 \pm 10\%_{max}$) and control arms ($78 \pm 10\%_{max}$; $P = 0.59$). In support of our hypothesis, Na^+ concentration was elevated following I/R injury, but likely not accompanied by alterations in cutaneous microvascular function.

NEW & NOTEWORTHY In the present study, we have demonstrated that sweat sodium concentration is elevated following ischemia-reperfusion injury during passive heat stress. This does not appear to be mediated by reductions in cutaneous microvascular function or active sweat glands, but may be related to alterations in local sweating responses during heat stress. This study demonstrates a potential use of eccrine sweat glands to understand sodium handling following ischemia-reperfusion injury, particularly given the challenges of in vivo studies of renal ischemia-reperfusion injury in humans.

ischemia-reperfusion injury; microvascular function; sweat gland; sweat electrolytes; sweat

INTRODUCTION

Kidney injury is a major cause of hospitalization during heat waves (1). This injury is hypothesized to be mediated by heat stress (coinciding with dehydration) that results in localized ischemia-reperfusion (I/R) injury (2). Localized ischemia is likely caused by reductions in kidney blood flow, particularly in the renal cortex (3), that occurs concomitantly with an increased energetic demand to increase sodium reabsorption in the renal tubules (4). This results in a low ATP environment that can induce oxidative stress and inflammation, giving rise to an increase in the risk of kidney injury (5), particularly when perfusion is reestablished (2). The clinical criteria defining kidney injury is a reduction in glomerular filtration rate and urine output (6). However, these are hallmark responses of the effect of heat stress on the kidneys in the absence of injury (2). Nevertheless, the proposed kidney pathophysiology during heat stress is relatively similar to renal I/R injury in the absence of heat stress (7, 8). A regular observation in the context of normothermic renal I/R injury in clinical settings is an increase in the fractional excretion of sodium, which is interpreted as reductions in tubular sodium reabsorption (9, 10). These observations are mechanistically supported by data obtained from rodent models that demonstrate that impaired tubular sodium reabsorption post-I/R injury is due to a reduction in the active transport of sodium (i.e., Na^+-K^+-ATPase availability) (11–13).

Correspondence: Z. J. Schlader (zschlade@iu.edu).
Submitted 20 November 2022 / Revised 20 March 2023 / Accepted 6 April 2023

It remains unknown if heat stress-mediated renal I/R injury causes impairments in sodium reabsorption. Filling this knowledge gap is important because: *1*) such understanding could help differentiate kidney pathophysiology from normal physiological responses to heat stress and *2*) impaired sodium reabsorption has potential ramifications on the ability of the kidneys to promote fluid conservation during heat exposure where body water loss would be expected due to sweating (2).

Given the anatomical and practical challenges of studying the kidneys in vivo in humans, human skin has been proposed as a model for understanding kidney function in response to heat stress (14). Specifically, it has been proposed that the eccrine sweat glands may be an experimental model for nephrons given the anatomical and functional similarities (15, 16). For example, sweat glands have been observed to excrete metabolites (e.g., urea) in end-stage renal disease, seemingly in compensation for compromised kidney function (16). Moreover, the eccrine sweat glands contain sodium [Na^+]/potassium [K^+] pumps that actively reabsorb sodium in the proximal segment of the eccrine duct (15, 16). With this background, the primary aim of the present study was to use eccrine sweat glands as a model to understand the impact of I/R injury on sodium reabsorption in humans. To this end, we tested the hypothesis that sweat sodium concentration would be elevated following I/R injury during whole body passive heat stress. The testing of this hypothesis would serve to establish a model that future studies could leverage to understand the mechanisms of impaired tubular reabsorption of sodium in humans.

I/R injury blunts the cutaneous vasodilatory response to local heating in healthy humans likely due to impairments in endothelial function secondary to oxidative stress (17). However, no study has examined the cutaneous vascular responses following I/R injury during passive heat stress. Such information may provide mechanistic insights underlying potential differences in sweat sodium concentrations following I/R injury. Therefore, the secondary purpose of the present study was to assess the impact of I/R injury on cutaneous microvascular responses during passive heat stress. We tested the hypothesis that the cutaneous vasodilatory response to local heating during passive heat stress would be impaired following I/R injury.

METHODS

The study was approved by the Institutional Review Board at Indiana University (IRB# 2010183521). The study conformed to the Declaration of Helsinki, except for registration in a database. Before participating in any study-related activities, each subject was fully informed of the experimental procedures and possible risks before providing informed written consent.

Subjects

To our knowledge, there are no direct data to inform differences in sweat electrolytes following an I/R injury to determine the sample size required for adequate statistical power a priori. That said, previous work has identified that the cutaneous microvascular responses to local skin heating are reduced following an experimental I/R injury (17), which is a secondary purpose of the present study. Therefore, the effect size was calculated based on data demonstrating that maximum cutaneous vascular conductance (CVC) is decreased following I/R injury by 0.55 ± 0.53 perfusion units-×mmHg (17) (dz = 1.04). Ten subjects were required to achieve power = 0.80 with α = 0.05 (G-Power v. 3.1.9.4). However, following the completion of 10 subjects, we were underpowered to identify changes in sweat sodium concentration and or differences between the control and experimental (i.e., I/R) arms due to inadequate sweat volume collected necessary for sweat electrolyte analyses (i.e., three out of 10 subjects had inadequate sweat volume collected). Therefore, we collected data in an additional five subjects to ensure that we would have 10 complete data sets for sweat electrolyte analyses.

Fifteen healthy subjects completed the study and subject characteristics are presented in Table 1. All subjects self-reported to be nonsmokers, not taking medications, and free of any known cardiovascular, metabolic, neurological, or renal diseases. In addition, subjects were not heat acclimated and self-reported to regularly engage in physical activity. Female subjects were not pregnant as confirmed through a urine pregnancy test before each visit, self-reported to be normally menstruating, and had no diagnosis of a menstrual cycle-specific disorder. Due to the cross-body experimental design, women were tested at any point during their menstrual cycle. Similarly, diet and/or sodium intake was not controlled in the present study, except subjects were instructed to avoid exercise alcohol, and caffeine for at least 12 h before arrival at the laboratory, and all subjects were instructed to eat a light meal ~2 h before arriving.

Experimental Protocol

Subjects visited the laboratory on two occasions separated by at least 24 h. The first visit involved screening and the second was the experimental trial. Subjects completed the single experimental trial using a cross-body design (i.e., a control and experimental arm assigned via block randomization; Fig. 1). All experimental trials were completed throughout the calendar year (2020–2021) in Bloomington, IN—a climate that has been shown to induce minimal heat acclimatization (18). The timeline of the experimental protocol is presented in Fig. 2.

Upon arrival, subjects provided a urine sample by completely voiding their bladder in a collection urinal. Subjects were confirmed to be euhydrated defined as a urine-specific gravity $\leq$ 1.020 (1.010 ± 0.006) (19). Following urine collection,

Table 1. *Subject characteristics measured during Visit 1 (screening)*

Subject Characteristics	
Men	*n* = 5
Women	*n* = 10
Age, yr	25 [20, 32]
Height, cm	171 [156, 191]
Body mass, kg	70 [52, 93]
Body mass index, kg/m^2	24 [19, 32]
Body surface area, m^2	1.8 [1.5, 2.2]

Data are presented as mean [min, max].

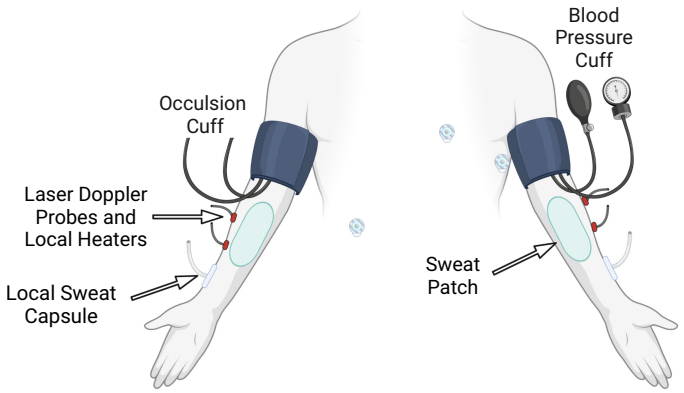

Figure 1. Schematic of the experimental set-up. The cross-body experimental design was carried out by randomly assigning an experimental arm (*right arm above*) and control arm. On the experimental arm, an occlusion cuff was placed around the upper arm and on the control arm, a blood pressure cuff was placed around the upper arm. On dorsal aspect of each forearm, local sweat capsules were secured at the most distal point just proximal to the wrist. Similarly, on the dorsal aspect of each forearm, two local heating units and laser Doppler flowmetry probes were secured each [distal for local heating to 39°C (40 min) and 44°C (20 min); proximal for control site and local heating to 44°C (20 min)]. Sweat was collected via absorbent patches placed on the ventral aspect of each forearm. Image created with BioRender and published with permission.

subjects were weighed nude, instrumented, and then donned the water-perfused suit.

Subjects were positioned supine on a comfortable patient table with their arms flat on the table positioned at ~45° laterally from their torso and forearms dorsal side up in a temperate thermal environment (~22°C, 55% relative humidity). A 30-min thermoneutral baseline was completed by perfusing 34°C water through the water-perfused suit. Following this baseline period, the water temperature was rapidly switched to 50°C, which commenced the ~160 min passive heating protocol. After the onset of sweating and ~30 min into passive heating, an absorbent patch was applied (as indicated below) to the ventral aspect of each forearm for sweat collection.

On the experimental arm, following sweat collection and ~60 min of passive heating (core temperature: 37.8 ± 0.3°C), subjects underwent 20 min of experimental ischemia, administered by a cuff wrapped around the upper arm and held constant at a pressure of 220 mmHg (E20 Rapid Cuff Inflator, Hokanson Inc., Bellevue, WA). After 20 min of occlusion, the cuff was released and subjects rested during a 20-min reperfusion period. This I/R protocol has been previously used in our laboratory (20) and others (17). Following the reperfusion period, a second absorbent patch was applied to each forearm for sweat collection. Simultaneously, the skin on both the control and experimental arm was heated locally to a temperature of 39°C (distal local heaters) for 40 min and then both the distal and proximal local heaters on each arm were increased to 44°C for 20 min. Importantly, while sweat collection occurred without local heating before the I/R protocol, we had no evidence that local heating a small area of skin on the dorsal side of the forearm influences sweating on the ventral side of the forearm.

Active sweat gland measurements (via modified iodine technique, see *Instrumentation and Measurements*) were taken at the end of the initial 60-min passive heating period (i.e., before the I/R protocol), immediately following the I/R protocol, and every 20 min during the local heating protocol.

Instrumentation and Measurements

Height was measured with a custom stadiometer and body mass was measured with a calibrated scale (ScaleTronics 5201, Welch-Allyn, Chicago, IL). Brachial blood pressure was measured on the control arm via electrosphygmomanometry (Tango M2; SunTech, Raleigh, NC) and mean arterial pressure (MAP, mmHg) was calculated as diastolic pressure plus one-third pulse pressure and reported every 20 min. Heart rate (beats/min) was continually measured via a 3-lead ECG (Datex-Ohmeda, Helsinki, Finland) and reported

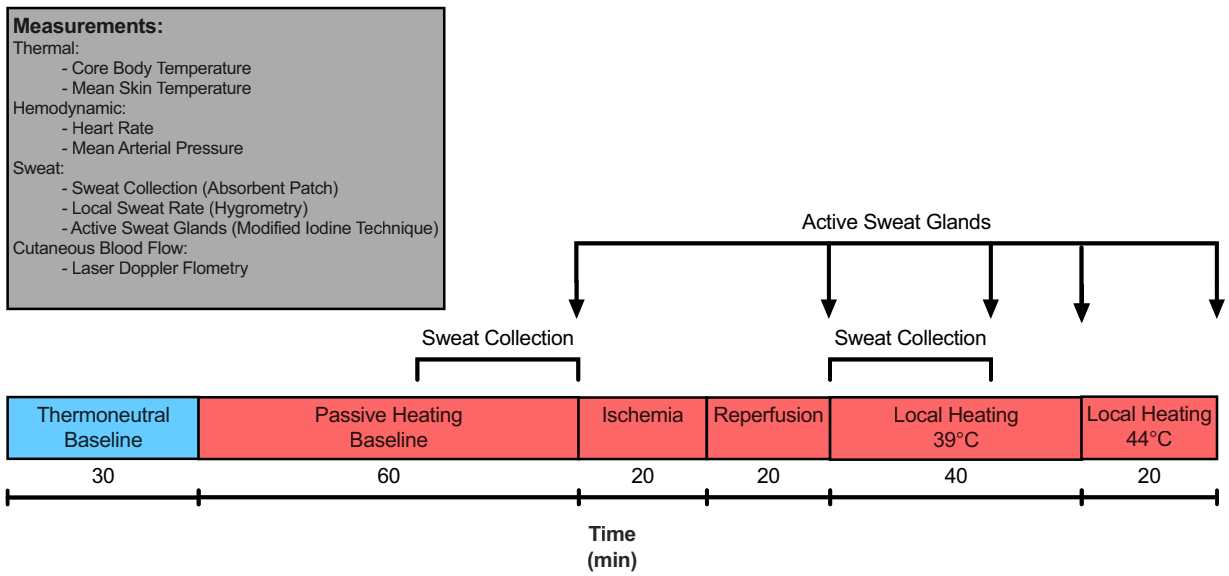

Figure 2. Schematic of the experimental protocol timeline and measurements. The thermoneutral baseline (blue) and whole-body passive heating (red) were completed by perfusing 34°C and 50°C water (respectively) through a water-perfused suit.

every 20 min. Core temperature (°C) was measured via a telemetry pill that each subject swallowed ~6–8 h before the experimental trial (n = 4) (21) or via a self-inserted rectal temperature probe inserted ~10 cm beyond the sphincter if the subject was contraindicated to consuming the telemetry pill or they voluntarily elected to utilize the rectal temperature probe (n = 11). Core temperature is reported at the end of the thermoneutral baseline and every 20 min throughout the experimental protocol. Thermocouples (Omega Technologies, Inc., Westlake Village, CA) were used to measure mean skin temperature (°C), which was calculated as the weighted average of four skin locations (right chest, triceps, thigh, and calf) (22) and reported every 20 min. Body temperature was controlled with a tube-lined water-perfused suit (Med-Eng, Ottawa, ON, Canada) that covered the entire body except for the head/neck, hands, and feet. In addition, to augment the rate of increase in core temperature, solar and fleece blanket were layered on the subjects' torso and legs.

Local skin heaters (Moor Instruments, Devon, UK) covering an area of 11 mm^2 were placed on two sites of the right and left dorsal forearm. Red blood cell flux (PU), an index of skin blood flow, was measured at each site using integrated laser Doppler flowmetry probes (Moor Instruments, Devon, UK), which were seated in the center of each local heater. Local forearm skin temperature was measured via temperature probes embedded in the local heating units (Moor Instruments, Devon, UK).

Sweat was collected via an absorbent patch that comprised sterile gauze (surface area: 77 cm^2) secured to the skin via impermeable Tegaderm (3 M Medical Sciences, St. Paul, MN) on the ventral aspect of each forearm after the skin was cleaned with deionized water and sterile gauze. The absorbent patch was removed once saturated with sweat (experimental arm: pre-I/R: 24 ± 3 min, post-I/R: 31 ± 7 min; control arm: pre-I/R: 25 ± 4 min, post-I/R: 29 ± 6 min) and placed directly into the sterile syringe for weighing and sweat extraction. Sweat was extracted by plunging the absorbent patch in a sterile syringe (23) into an Eppendorf microcentrifuge tube and stored at room temperature (~22°C) for later analyses, which were conducted within the same day of the experimental trial. Sweat electrolytes (sodium [Na^+], potassium [K^+], chloride [Cl^-]) were analyzed in duplicate via an electrolyte analyzer (EasyLyte Plus; Medica Corporation, Bedford, MA). The EasyLyte Plus uses a direct measurement ion selective electrode and the manufacturer's specifications report a coefficient of variation of <1% for within-day sample analyses and an accuracy range of 25–1000 mmol/L at a correlation coefficient of 1.00. Finally, due to the inability to extract enough sweat volume for analyses in four subjects, sweat electrolytes are reported for 11 subjects (n = 7 women).

Local sweat rate was measured by tightly securing a capsule that covered 3.9 cm^2 of the skin on the dorsal surface of each forearm, ~3 cm below where the distal local heaters and laser Doppler probes were placed. The capsule was tightly taped to the skin after applying it with double-sided adhesive. Dry nitrogen was perfused through the capsule at a rate of 0.5 L/min. The water vapor from the skin exiting the gas capsule was continuously measured by capacitance hygrometry (HMT130, Vaisala, Woburn, WA). Local sweat rate was calculated by multiplying the humidity output by the flow rate of the dry nitrogen and dividing that value by the surface area of the capsule. Local sweat rate data are reported every 20 min throughout the protocol and as an average during the sweat collection periods pre- and post-I/R. Estimated whole body sweat loss and percent changes in body mass were calculated from the change in nude body mass pre- to posttrial (n = 14 due to a missed recording of one posttrial nude body mass).

The number of active sweat glands was determined using the modified iodine-paper technique previously described (24). Briefly, ~48 h before an experimental trial, pieces of 100% cotton paper (32 lb. 100% cotton paper; Southworth, Neenah, Inc., Atlanta, GA) were cut into predetermined size (3.9 cm^2; i.e., the same surface area as used in the measurement of local sweat rate) and placed in a sealed container suspended above iodine in solid form to avoid direct contact with the iodine. After ~48 h, the pieces of paper became saturated with iodine and subsequently transferred to a sealed, sterile Petri dish for use during the experimental protocol. Before the application of the cotton paper, the skin was blotted dry and the cotton paper was firmly pressed against the skin surface for a period of ~3–5 s. With this technique, sweat excreted from the active sweat glands form identifiable blue dots on the iodine-saturated paper when it is placed in contact with the skin surface. After the paper was removed from the skin, an image was immediately taken (iPhone 12 Pro Max, Apple Inc., Cupertino, CA). Image processing and analysis (i.e., for count of active sweat glands) were completed using ImageJ (a public domain Java image processing and analysis program: https://imagej.nih.gov/ij/) according to the step-by-step instructions provided in Appendix A by Gagnon et al. (24). A representative image of active sweat gland count is presented within Fig. 5*E*. Due to technical issues with image quality, there are missing data for active sweat glands on the experimental arm (pre-I/R: n = 13; post-I/R: n = 10; 20 min post-I/R: n = 10; 40 min post-I/R: n = 10; 60 min post-I/R: n = 7) and control arm (pre-I/R: n = 15; post-I/R: n = 14; 20 min post-I/R: n = 13; 40 min post-I/R: n = 10; 60 min post-I/R: n = 11). Finally, total active sweat gland count was normalized to surface area (i.e., glands per cm^2), which permitted the calculation of active sweat gland output (i.e., local sweat rate [mL/min/cm^2] divided by glands per cm^2).

Data and Statistical Analyses

Data that were collected during the local heating at 39°C and 44°C were visually inspected to ensure that a plateau in red blood cell flux was observed, which was the case in all instances. CVC (PU/mmHg) was calculated as red blood cell flux divided by the mean arterial pressure. Red blood cell flux and CVC were then represented as a percentage of the maximum local heating-induced vasodilatory response as identified during heating at 44°C (i.e., red blood cell flux [$\%_{max}$] and CVC [$\%_{max}$]) (25).

To our knowledge, experimental I/R has not been used during whole body passive heat stress. Therefore, to characterize and quantify the stimulus (i.e., I/R injury) we compared second-to-second red blood cell flux data from the present study to previous work in our laboratory (20) that used the same experimental protocol, but under thermoneutral conditions. Fourteen healthy adults (age: 25 ± 3 yr, body mass index:

24.6 ± 3.6 kg/m^2), including six women in which menstrual cycle was controlled (i.e., within the first 10 days of menstruation), completed the previous study (20). First, we have provided a visual characterization of the continuous red blood cell flux (%$_{max}$) responses during the final 5 min of ischemia and the 20-min reperfusion period. Second, we calculated the peak red blood cell flux (%$_{max}$) occurring during the 20-min reperfusion period. Third, to quantify the initial reactive hyperemic response during the reperfusion period, we calculated the area under the curve during the first 5 min of reperfusion relative to the preischemia red blood cell flux in the present study (mean: 67%$_{max}$) and under thermoneutral conditions (mean: 7%$_{max}$). Finally, we calculated the area under the curve during the entire 20-min reperfusion period. Peak red blood cell flux and the area under the curve data were analyzed via two-tailed unpaired *t* tests.

Continuously collected data (i.e., mean skin temperature, heart rate, local sweat rate, red blood cell flux) were sampled at 1,000 Hz via a data acquisition system (PowerLab 16/35, ADInstruments). All data were analyzed using GraphPad Prism v. 9.4.1 (GraphPad Software Inc., La Jolla, CA). A priori statistical significance was set at $P \leq 0.05$, and exact *P* values are reported where possible. Data are reported as means ± SD, along with 95% confidence intervals (95% CIs) for sweat electrolytes. Whole body responses to passive heat stress (core temperature, mean skin temperature, heart rate, and mean arterial pressure) were analyzed using a one-way analysis of variance (ANOVA). Active sweat glands, local sweat rate, red blood cell flux, and cutaneous vascular conductance were analyzed using a repeated-measures linear mixed-effects model (time × arm). Prior to statistical analyses and after visual inspection of the predicted and actual residuals (i.e., QQ plots), it was determined that sweat electrolyte data were not normally distributed. All other data were normally distributed. Statistical inference of sweat electrolytes was therefore completed after log transformation of the data before statistical analyses, which normally distributed the data. The [LOG] of sweat electrolytes were analyzed using a repeated-measures linear mixed-effects model (time × arm) and using a two-tailed paired *t* test. When applicable, the Geisser-Greenhouse correction was applied if sphericity could not be assumed. The cutaneous vascular response to local heating was also analyzed using a two-tailed paired *t* test. Baseline red blood cell flux and cutaneous vascular conductance were analyzed via two-tailed *t* tests. Finally, if a significant interaction or main effect was found (26), post hoc analyses were completed using Šídák's multiple comparisons tests.

RESULTS

Whole Body Responses to Passive Heat Stress

Whole body responses to passive heat stress are presented in Fig. 3, *A–D*. Briefly, core temperature (Fig. 3*A*) increased from 0 min (37.1 ± 0.2°C) at 40 min (37.4 ± 0.2°C; $P < 0.0001$) and remained elevated for the remainder of the passive heating period (all $P < 0.0001$). The peak increase in core temperature was +1.5 ± 0.2°C. Similarly, mean skin temperature (Fig. 3*B*) was elevated from 0 min (34.6 ± 0.9°C) at 20 min (37.8 ± 0.8°C; $P < 0.0001$) and remained elevated for the remainder of the passive heating period (all $P < 0.0001$). Heart rate (Fig. 3*C*) increased from 0 min (66 ± 13 bpm) at 40 min (87 ± 16 bpm; $P = 0.0068$) and remained elevated for the remainder of the passive heating period (all $P < 0.0001$). Mean arterial pressure (Fig. 3*D*) did not change from 0 min at any timepoint during the passive heating period ($P \geq 0.4350$). Pre- and posttrial body mass was 69.2 ± 12.9 kg and 67.7 ± 12.7

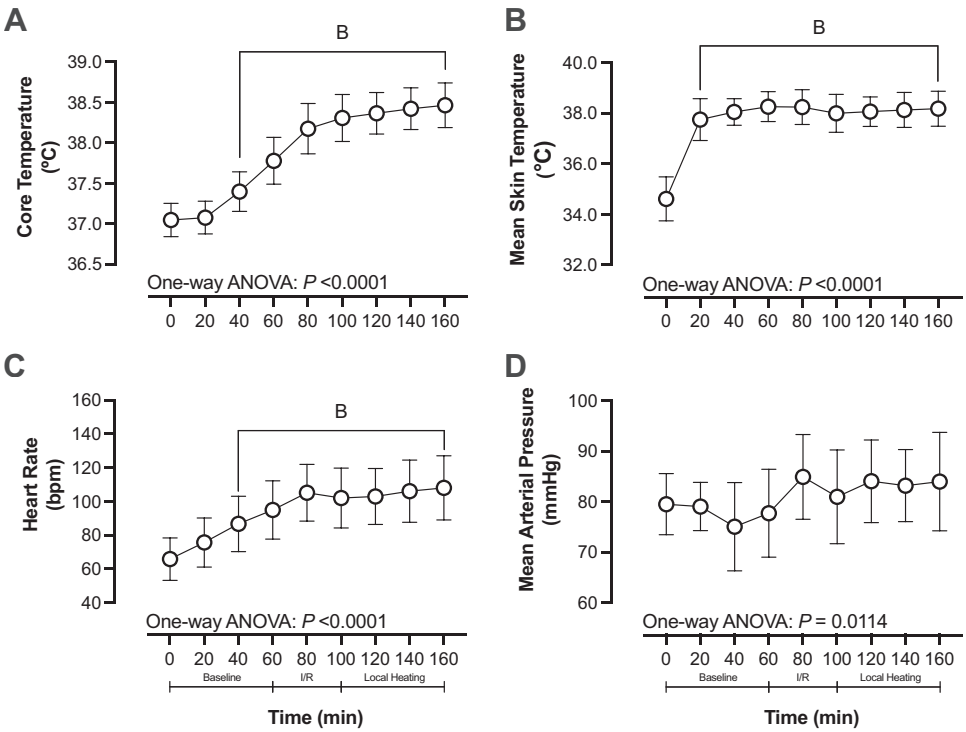

Figure 3. Core temperature (*A*), mean skin temperature (*B*), heart rate (*C*), and mean arterial pressure (*D*) responses to 160 min of whole-body passive heating via water-perfused suit (50°). Data are presented as means ± SD. *n* = 15 (5 men, 10 women). All data were analyzed via one-way analysis of variance. If significant ($P < 0.05$), post hoc analyses were completed using Šídák's multiple comparisons tests. B, different from 0 min ($P < 0.05$).

kg, respectively. Percent change in body mass from pre- to posttrial was −2.1 ± 0.7% and estimated whole-body sweat rate was 0.4 ± 0.1 L/h.

Ischemia-Reperfusion Injury: Reactive Hyperemia

A characterization of the I/R protocol during passive heat stress and thermoneutral conditions from a previous study in our laboratory conducted using the same I/R protocol and measurements, but in a different cohort of participants (20) is presented in Fig. 4*A*. Peak red blood cell flux ($\%_{max}$) during the 20-min reperfusion period is presented in Fig. 4*B*. Peak red blood cell flux was higher during passive heat stress (90 ± 11%; $P < 0.0001$) compared with thermoneutral conditions (63 ± 15%). The area under the curve in the first 5-min post-reperfusion relative to preischemia red blood cell flux, and the area under the curve across the entire 20-min reperfusion period relative to during ischemia is presented in Fig. 4, *C* and *D*, respectively. The area under the curve during the first 5 min of the reperfusion period in the thermoneutral condition, relative to preischemia red blood cell flux, was higher (6,953 ± 1,919 arbitrary units [AU]; $P = 0.0097$) than during passive heat stress (5,230 ± 1,390 AU). Conversely, the area under the curve across the entire 20-min reperfusion was higher during the passive heat stress (20,030 ± 2946 AU; $P < 0.0001$) compared with under thermoneutral conditions (9,442 ± 885 AU). This greater area under the curve across the entire 20-min reperfusion during passive heat stress was due to a sustained increase in red blood cell flux ($\%_{max}$) over time compared with the return of red blood cell flux to preischemia levels during reperfusion in thermoneutral conditions.

Local Sweat Responses

Local sweat rate is presented in Fig. 5, *A* and *B*. Local sweat rate (Fig. 5*A*) was not different between the experimental (0.03 ± 0.01 mL/min/cm^2) and control (0.03 ± 0.01 mL/min/cm^2; $P = 0.4521$) arms at the end of the thermoneutral baseline period (0 min). There was an interaction effect ($P < 0.0001$) for local sweat rate. Local sweat rate increased from 0 min in both arms ($P < 0.0001$), except for during ischemia on the experimental arm, which did not differ from the 0 min time point ($P = 0.0685$). Similarly, there were no differences between the experimental and control arms at any time point except for during the ischemia (experimental arm: 0.4 ± 0.5 mL/min/cm^2; control arm: 1.3 ± 0.4 mL/min/cm^2; $P = 0.0004$). In contrast, when local sweat rate is reported as a mean during the sweat collection periods pre- and post-I/R (Fig. 5*B*), there was a significant interaction effect ($P = 0.0008$). Mean local sweat rate increased from pre- to post-I/R in the control arm (pre: 0.9 ± 0.3 mL/min/cm^2; post: 1.2 ± 0.4 mL/min/cm^2; $P = 0.0010$), but not in the experimental arm (pre: 1.0 ± 0.4 mL/min/cm^2; post: 1.0 ± 0.4 mL/min/cm^2; $P = 0.8590$). In addition, mean local sweat rate was higher in the control arm compared to the experimental arm post-I/R ($P = 0.0094$).

A representative image of active sweat gland count from pre to post-I/R and between control and experimental arms is presented in Fig. 5*E*. Active sweat glands (i.e., count per cm^2, and sweat output per gland) measured on the experimental and control arms immediately before and after the I/R protocol and every 20 min following the end of the 20 min reperfusion are presented in Fig. 5, *C* and *D*. There was no effect of I/R on active sweat glands density (interaction

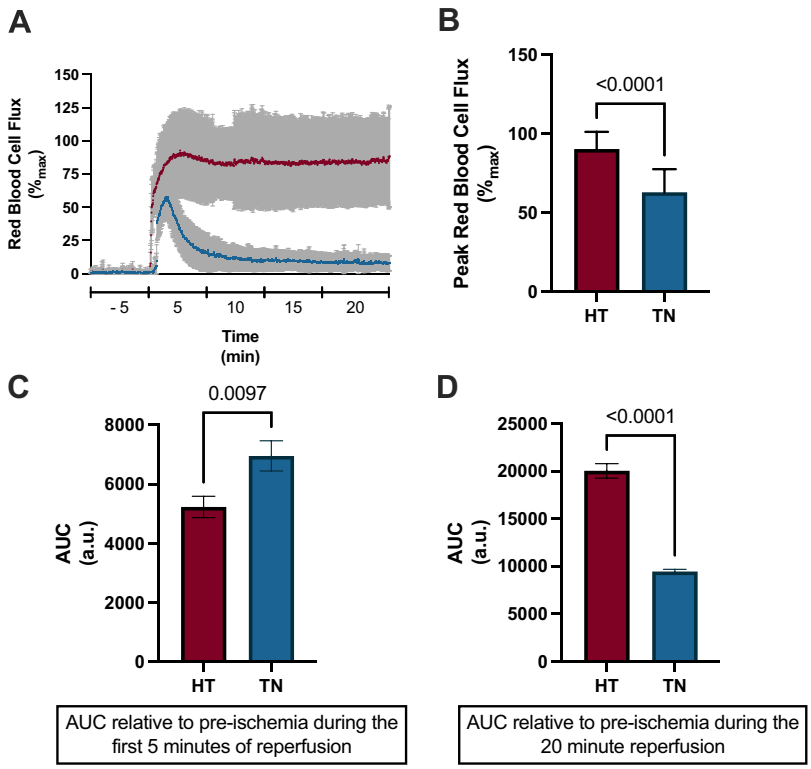

Figure 4. A comparison of red blood cell flux responses during the final 5 min of ischemia and the 20-min reperfusion period during passive heat stress (HT; red) and under thermoneutral conditions (TN; blue) from Greenshields et al. (20). *A*: a characterization of the second-second red blood cell flux (as a percentage of max) responses during the final 5 min of ischemia and the 20-min reperfusion. *B*: peak red blood cell flux representative of the reactive hyperemia following reperfusion presented as a percentage of max during the 20-min reperfusion period. *C*: area under the curve (AUC; AU) during the first 5 min of reperfusion relative to the preischemia red blood cell flux (HT: 67%$_{max}$; TN: 7%$_{max}$). *D*: AUC during the entire 20-min reperfusion period relative to the preischemia red blood cell flux (HT: 67%$_{max}$; TN: 7%$_{max}$). Data are presented as means ± SD. Data in *B*–*D* were analyzed via unpaired *t* tests and exact *P* values reported.

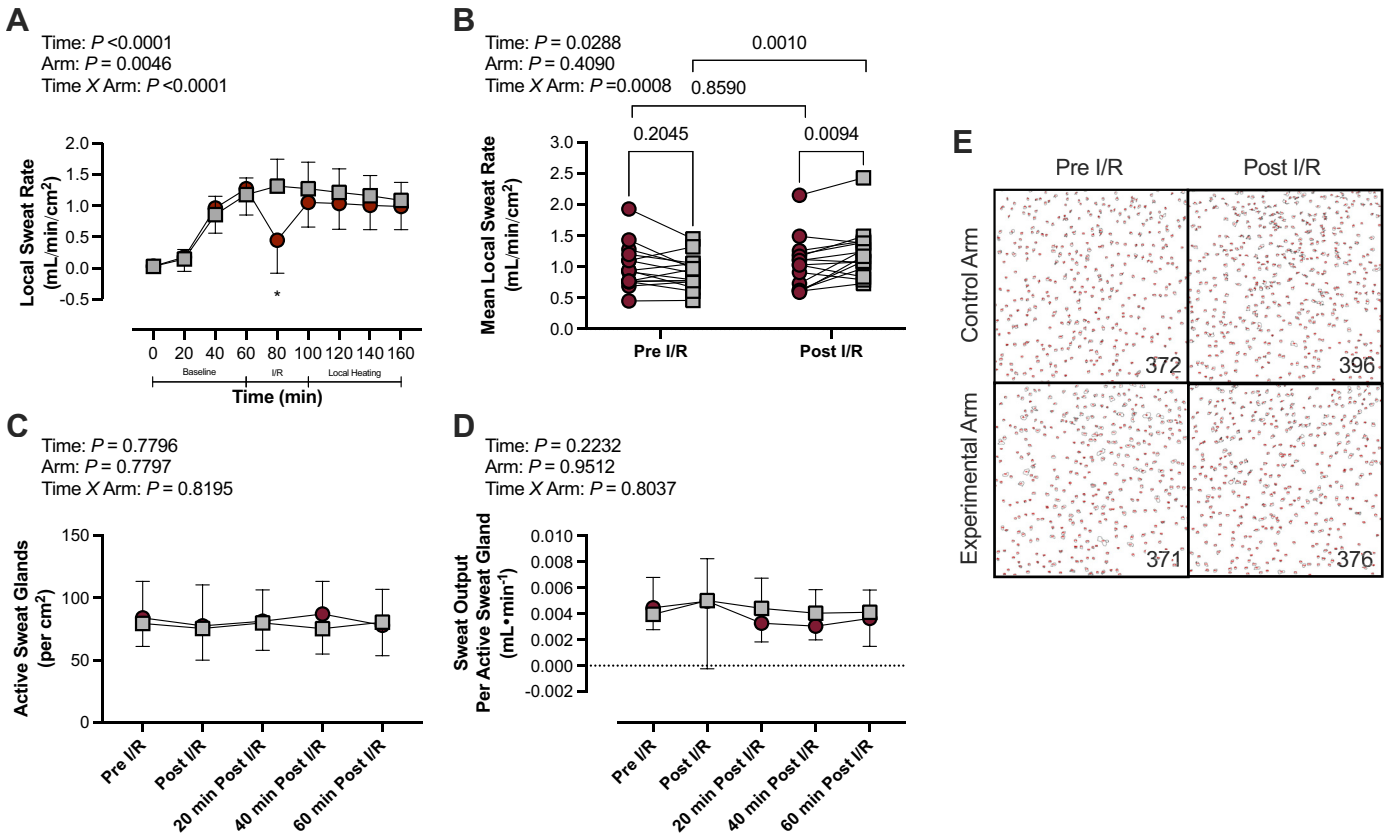

Figure 5. Local sweat rate and active sweat gland responses during the passive heating protocol. Data are presented for the experimental arm (red circles) and control arm (grey squares) as means ± SD or as individual data. *A*: local sweat rate presented at the end of the thermoneutral baseline (0 min) and every 20 min thereafter. *B*: mean local sweat rate calculated during the sweat collection period pre and post ischemia-reperfusion (I/R). *C*: active sweat glands (glands per cm^2) measured before (pre) and immediately after (post) I/R, and every 20 min during the local heating protocol. *D*: sweat output per gland [mL/min] measured before (pre) and immediately after (post) I/R, and every 20 min during the local heating protocol. *E*: a representative image of active sweat gland count (bottom right of each quadrant) from pre to post I/R and between control and experimental arms. Finally, a representative image of active sweat gland count is located in the *bottom left*. Total count is indicated in the bottom right of each quadrant. $n = 15$ (10 women, 5 men) for the local sweat rate data in *A* and *B*. There were missing data for the active sweat glands data in *C* and *D* in the experimental arm (pre-I/R: $n = 13$; post-I/R: $n = 10$; 20-min post-I/R: $n = 10$; 40-min post-I/R: $n = 10$; 60-min post-I/R: $n = 7$) and control arm (pre-I/R: $n = 15$; post-I/R: $n = 14$; 20 min post-I/R: $n = 13$; 40-min post-I/R: $n = 10$; 60-min post-I/R: $n = 11$). Data were analyzed using a repeated measures linear mixed model (time × arm) and exact *P* values shown where possible. The linear mixed model table is shown. If a significant interaction or main effect was found, post hoc analyses were completed using Šídák's multiple comparisons tests. *Different from control arm ($P < 0.05$).

effect: $P = 0.8195$) or sweat output per gland (interaction effect: $P = 0.8037$).

Sweat Electrolyte Concentrations

Summarized raw data for all sweat electrolytes are presented in Supplemental Table S1 (https://doi.org/10.5281/zenodo.7709477). Log-transformed sweat electrolyte data for Na^+, K^+, and Cl^- measured before and after the I/R protocol are presented in Fig. 6, *A–C*. Briefly, sweat Na^+ increased from pre-I/R in the experimental arm ($P = 0.0492$), but not in the control arm ($P = 0.4542$). The change in sweat Na^+ from pre- to post-I/R was greater in the experimental arm compared to the control arm (experimental arm: $+0.97$ [$+0.67$ – 1.27] [LOG] Na^+; control arm: $+0.68$ [$+0.38$ – 0.99] [LOG] Na^+; $P = 0.0053$). It is important to note that this analysis contains two participants with a striking reduction in sweat Na^+ on the control arm (shown as diamond and triangle symbols in right panel of Fig. 6*A* and *B*) and finding that would not be expected and therefore are likely potential outliers. Even with one or both of these outliers removed, the change in sweat Na^+ was still greater in the experimental arm compared to the control arm ($P = 0.0128$ and $p = 0.0160$, respectively).

Cutaneous Microvascular Function

Cutaneous microvascular responses are presented in Fig. 7, *A–F*. Briefly, there were no differences in red blood cell flux (PU or $\%_{max}$) or CVC (PU/mmHg or $\%_{max}$) between the experimental and control arms at any point except for during ischemia (all $P < 0.0001$). Similarly, CVC ($\%_{max}$) during the local heating to 39°C (Fig. 7*E*; a marker of primarily nitric oxide-mediated cutaneous vasodilation) was not different between the experimental (80 ± 10%) and control arms (78 ± 10%; $P = 0.4999$). Interestingly, at the proximal local heaters (Fig. 7*F*; not heated to 39°C), CVC ($\%_{max}$) was similar to that measured at the distal local heaters (i.e., heated to 39°C) in the experimental (78 ± 11%) and control arms (76 ± 11%). This was likely mediated by the local skin temperature (in the absence of local heating) that was ~36 ± 1°C.

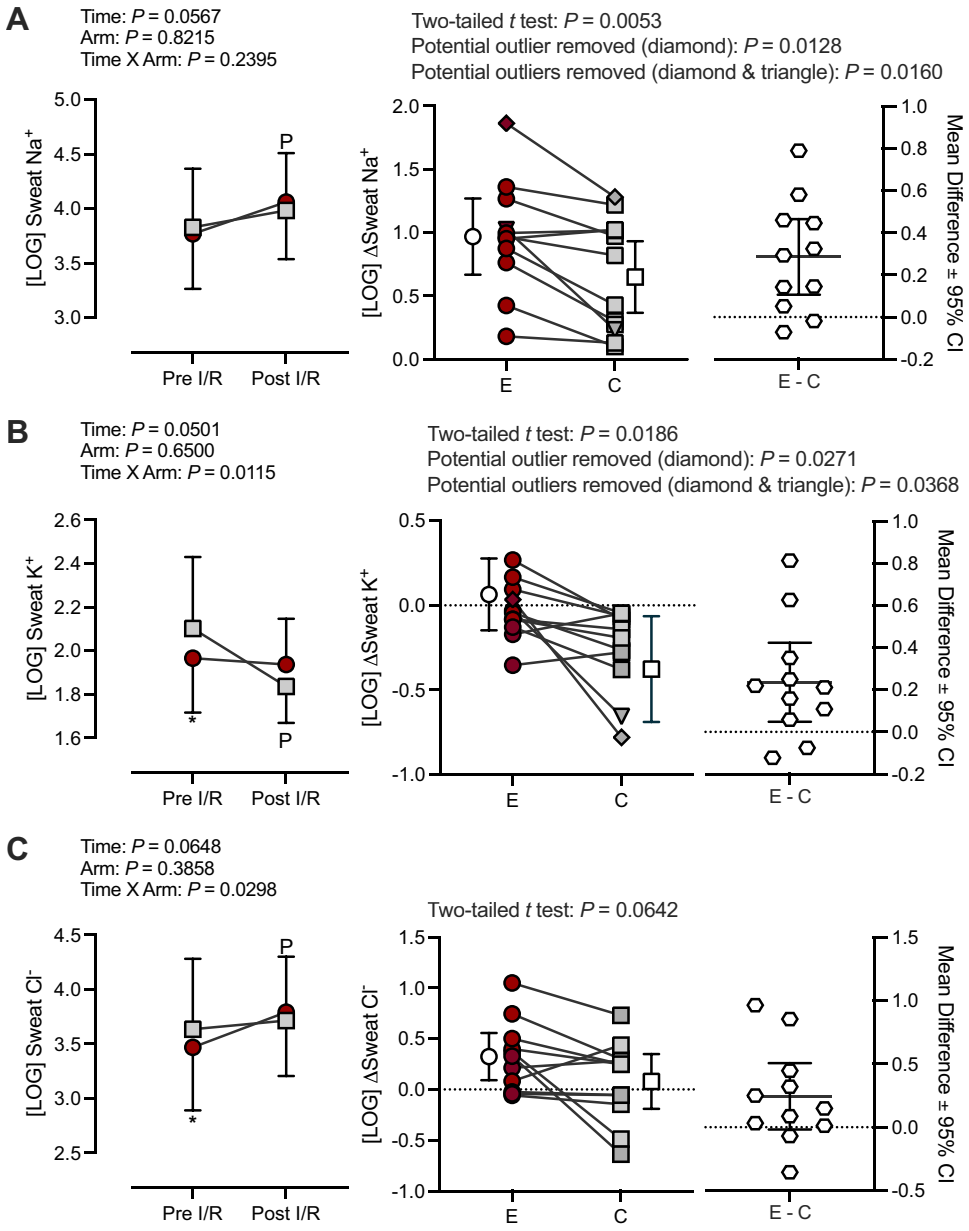

Figure 6. Sweat electrolytes measured from sweat collected on the experimental arm (red circles) and control arm (gray squares) before (pre) and after (post) the I/R. Sweat sodium (Na^+), potassium (K^+), and chloride (Cl^-) are presented in *A*–*C*, respectively. Data are presented following log transformation as means ± SD (*left column*), as an absolute change from pre I/R as means ± SD (open circle and square for the experimental and control arms, respectively) and as individual data (*middle column*), or as the mean difference between the experimental and control arms ±95% confidence interval (CI; *right column*). All statistical inference was completed after data were log transformed and analyzed with a repeated-measures linear mixed-effects model (*left column*) or a two-tailed *t* test (*middle column*). n = 11 (7 women, 4 men). Exact P values are shown. If a significant interaction or main effect was found, post hoc analyses were completed using Šídák's multiple comparisons tests. P, different from pre I/R ($P < 0.05$). *Different from control arm ($P < 0.05$).

DISCUSSION

Given the challenges of examining intrinsic mechanisms of impaired renal tubular function following ischemic kidney injury in vivo in humans, we aimed to utilize a noninvasive, experimental model in humans to identify the implications of I/R injury on tubular reabsorption of sodium by leveraging the anatomical, physiological and functional similarities between nephrons and eccrine sweat glands. Thus, the primary purpose of the present study was to test the hypothesis that sweat sodium concentration would increase following I/R during passive heat stress. In support of this hypothesis, we demonstrate that sweat sodium concentration is elevated following I/R injury compared to the control arm (Fig. 6*A*). In contrast to our secondary hypothesis, this elevation in sweat sodium concentration is not accompanied by alterations cutaneous microvascular function (Fig. 7, *A*–*F*).

Ischemia-Reperfusion Injury: Reactive Hyperemia

To our knowledge, this is the first study to use an I/R protocol during whole body passive heating. Therefore, it was necessary to quantify the magnitude of the stimulus (i.e., reactive hyperemia). To do this, we compared the red blood cell flux responses during the 20-min reperfusion period in the present study to data collected in a previous study in our laboratory (20). Preischemia red blood cell flux was ~67%$_{max}$ during passive heat stress in the present study and ~7%$_{max}$ under thermoneutral conditions, and upper arm occlusion during the 20-min ischemia period reduced red blood cell flux to ~0%$_{max}$ in both studies. Immediately upon reperfusion, peak red blood cell flux (Fig. 4*B*) was greater in the present study (~90%$_{max}$) compared to under thermoneutral conditions (~63%$_{max}$). This finding is unsurprising given the greater demand for skin blood flow during passive heat stress and the lower resistance

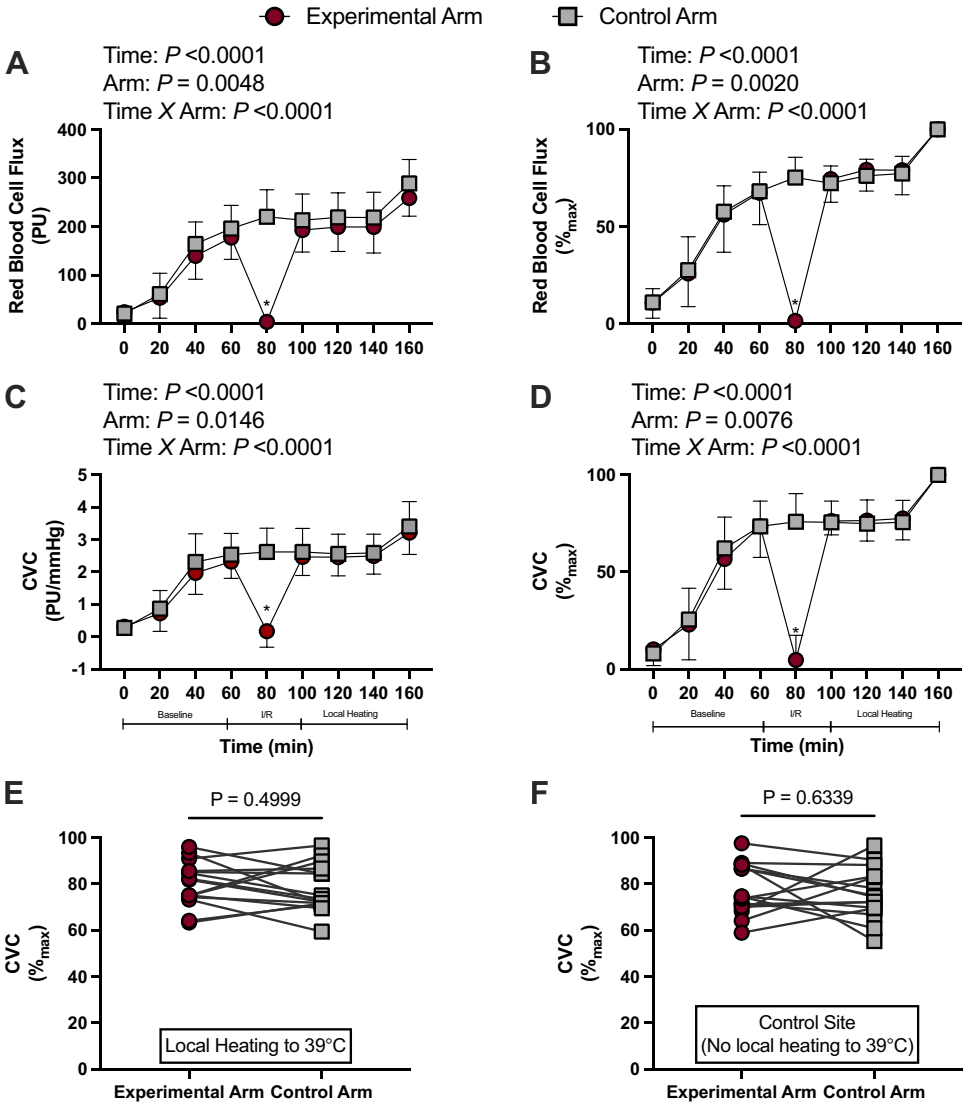

Figure 7. Red blood cell flux (PU; *A*), red blood cell flux (%max; *B*), cutaneous vascular conductance (CVC, PU/mmHg; *C*), and cutaneous vascular conductance (CVC, %max; *D*) presented before whole body passive heating (0 min) and every 20 min during the passive heating protocol (including the 60-min baseline, 40-min I/R protocol, and the 60-min local heating protocol (i.e., 40-min local heating to 39°C and 20-min local heating to 44°C. *E* and *F*: cutaneous vascular conductance (CVC, % max) during local heating. Data are presented for the experimental arm (red circles) and control arm (grey squares) as means ± SD in *A*–*D* and as individual values in *E* and *F*. Data in *A*–*D* were analyzed via mixed effects model (time × arm) and exact *P* values reported. Data in *E* and *F* were analyzed via paired *t* tests and exact *P* values reported. *Different from control arm ($P < 0.05$).

in this vascular bed (27), but may have resulted in a greater reperfusion (i.e., stimulus for injury). To further quantify the reactive hyperemia response, we calculated the area under the curve during the first 5 min of reperfusion (relative to preischemia skin blood flow levels, Fig. 4*C*) and across the entire 20-min reperfusion period (relative to preischemic skin blood flow levels, Fig. 4*D*). The area under the curve during the first 5 min was greater under thermoneutral conditions compared to responses observed in during passive heat stress in the present study (Fig. 4*C*). This potentially highlights a reduction in cutaneous microvascular function during heat stress as a greater increase in skin blood flow following ischemia is often considered to be indicative of a healthy vasculature (27). However, this finding more likely demonstrates a reduced capacity to further increase skin blood flow during passive heat stress beyond that required for thermoregulation (28). Finally, the area under the curve across the entire 20-min reperfusion period was greater during heat stress compared to under thermoneutral conditions. This was likely due to the relatively rapid decline in red blood cell flux towards preischemia values under thermoneutral conditions compared with the continued demand for high skin blood flow during whole-body passive heat stress. Together, the purpose of these analyses was to attempt to quantify the I/R injury and reactive hyperemia profiles. However, it remains difficult to interpret whether the cutaneous reactive hyperemia responses during heat stress are indicative of a more injurious profile, which will require further investigation.

Sweat Electrolytes Concentrations and Potential Mechanisms

The primary outcomes in the present study were the changes in sweat electrolyte concentration from pre- to post-I/R injury. Our primary finding was that sweat sodium concentration was elevated following I/R injury (Fig. 6*A*). Interestingly, we observed a decrease in sweat potassium concentration in the control arm from pre- to post-I/R. This finding is somewhat spurious and unexpected given that sweat potassium is relatively stable across time and at various sweating rates (29). However, this decrease in sweat potassium concentration occurred in the control arm of all 11 subjects—whereas sweat potassium did not change in the experimental arm—ruling out any likelihood of systematic or methodological error or sample contamination and/or evaporation. Despite

this fact, the physiological mechanism mediating this reduction remains elusive and requires additional study.

We also examined several potential mechanisms underlying our observation of elevations in sweat sodium concentration following I/R injury. First, we observed no changes in red blood cell flux (i.e., skin blood flow) or cutaneous vascular conductance following the I/R protocol (Fig. 7, *A–D*). Following ischemia, red blood cell flux and cutaneous vascular conductance rapidly recovered to the same levels observed in the control arm. Moreover, to assess cutaneous microvascular function following the 20-min reperfusion period, we used a local heating protocol to assess cutaneous microvascular function by locally heating the skin to 39°C (serving as a bioassay of nitric oxide-mediated cutaneous vasodilation) (30). There were no differences between the experimental and control arms in cutaneous vascular conductance after 40 min of locally heating the skin to 39°C (Fig. 7*E*). Initially, this was a surprising finding considering that previous work has demonstrated impaired cutaneous microvascular function (i.e., reduced cutaneous vascular conductance) following I/R (17). However, compared with the sites on both the experimental and control arms that were not locally heated to 39°C, cutaneous vascular conductance was comparable indicating that local heating to 39°C did not induce any additional cutaneous vasodilation (Fig. 7*F*). It is important to note that this finding is likely the result of the mechanisms mediating cutaneous vasodilation during whole-body passive heat stress. During passive heat stress, ~80%–90% of cutaneous vasodilation to increase skin blood flow for thermoregulation is sympathetically mediated (27), whereas when locally heating the skin (i.e., not during passive heat stress) cutaneous vasodilation is primarily the result of local factors (e.g., nitric oxide) (28). Therefore, local heating protocols (31) may not be an appropriate method for assessing cutaneous microvascular function during heat stress. Regardless, neither red blood cell flux (i.e., skin blood flow) nor cutaneous vascular conductance were altered following I/R and likely did not contribute to the observed increase in sweat sodium concentration.

Second, we measured local sweat rate given its relationship with sweat sodium concentration (29). To this point, as sweat rate increases there is an increase in the rate of sodium secretion and a decrease in sodium reabsorption (32). In the present study, we present two primary findings with regard to sweat rate. When presented over the duration of the experimental protocol, we observe no difference in local sweat rate between the experimental and control arms (Fig. 5*A*). We only observed a difference in local sweat rate during ischemia, which corroborates previous work demonstrating a fall in local sweating rate as a function of a reduction in skin blood flow (33). However, when mean local sweat rate is calculated at the time of sweat collection pre and post-I/R (Fig. 5*B*), we observed that sweat rate was increased from pre-I/R in only the control arm and that post-I/R mean local sweat rate was higher in the control arm compared to the experimental arm. Despite a comparatively lower local sweat rate following I/R in the experimental arm, we observed an increase in sweat sodium concentration—a finding opposite to a normal anticipated physiological response (i.e., a lower sweat rate results in a decrease in sweat sodium concentration via increased time for sodium reabsorption in the proximal duct). This finding is striking and likely reflects some level of sweat gland dysfunction with regard to the capacity to reabsorb sodium following the I/R injury.

Third, we measured active sweat glands (Figs. 5, *C–E*) via the modified iodine-paper technique to capture potential alterations in active sweat gland density (number of active sweat glands per cm^2) and sweat output per active sweat gland. I/R injury did not alter any parameter related to the active sweat glands. Thus, it is unlikely that any aspect of active sweat glands (density or output) mediated the increase in sweat sodium concentration following I/R.

Based on our data, it is unlikely that cutaneous microvascular function, or active sweat glands, as assessed herein, contributed to our observations of increased sweat sodium concentration following I/R injury. Moreover, the differential responses in mean local sweat rate between the experimental and control arms following the I/R protocol perhaps suggest that a few alternative mechanisms are at play. First, experimental models in rodents have provided the best evidence regarding the mechanism mediating impaired tubular sodium reabsorption and increased fractional excretion of sodium following renal I/R injury (9, 13). Notably, Van Why et al. (13) observed a steady decline of Na^+-K^+-ATPase (both α- and β-subunit proteins) from 15 min to 24 h following renal ischemia and indicated that the proximal tubules are the most susceptible to injury (i.e., the site of ~60% of sodium reabsorption in the nephron). It is then plausible to speculate that tubular sodium reabsorption following I/R injury is mediated by a reduction in the primary active transporters of sodium across the basolateral membrane. We speculate that this could be occurring in the eccrine sweat duct, but this remains unknown.

Sweat electrolyte concentration is relatively hypotonic due to the reabsorption of sodium and chloride (29). This is primarily mediated by active transport of sodium via Na^+-K^+-ATPase in the proximal segment in the eccrine duct, which is rich in mitochondria because of the energy needed for active transport (34). Thus, there is also potential for marked oxidative stress that could reduce the energy production via oxidative phosphorylation of plasma glucose necessary for active transport (35), which is a similar etiological mechanisms in kidney injury (2), but this remains unexplored.

Relevant in the context of passive heat stress and progressive dehydration (via prolonged sweating) in the present study, the activity of Na^+-K^+-ATPase is influenced by plasma aldosterone concentration and sweat gland sensitivity to aldosterone (36). It is unlikely that there were differences in exposure of plasma aldosterone to the sweat glands on the experimental arm given the cross-body experimental design. Although it is a possibility that the sensitivity to plasma aldosterone was reduced in the experimental arm following I/R, the potential mechanism for an alteration in sensitivity remains elusive. Moreover, it is well known that individual factors alter sodium reabsorption and sensitivity to aldosterone (e.g., acclimation and fitness status, diet). Again, however, the cross-body study design prevents any influence of individual factors on the increase of sweat sodium concentration on the experimental arm following I/R injury (which occurred in 9 out of 11 subjects; see Fig. 6*A*).

Finally, both cystic fibrosis transmembrane conductance regulator (CFTR) channels and epithelial sodium channels

(ENaC) impact of sodium and chloride reabsorption and final sweat sodium and chloride concentrations (37). Indeed, in individuals with less CFTR channels (often observed in cystic fibrosis) there is less electrolyte reabsorption (38). Importantly, there is a functional interaction between CFTR channels and epithelial sodium channels (ENaC), as ENaC activation is dependent on functioning CFTR (37). However, it is unlikely that I/R elicited a reduction in the abundance or function of CFTR, and subsequent action of the ENaCs over such a short period of time. Together, each of these potential physiological mechanisms for the resultant increase in sweat sodium concentration on the experimental arm following I/R injury needs to be elucidated by utilizing more invasive measurements (e.g., skin biopsy, intradermal microdialysis, etc.) to determine role of each of these potential pathways.

Considerations

Given the development of the novel experimental model employed in the present study, there are a number of considerations that warrant mentioning. First, the study was dependent on obtaining adequate sweat samples from subjects for electrolyte analyses, which ultimately posed to be a challenge. To elicit sweating in our subjects, we selected to use whole body passive heating via a water-perfused suit for two primary reasons: *1*) this is an internally valid method that can rapidly increase core body temperature (2) to elicit sweating at volumes adequate for collection and analysis, and *2*) passive heat stress represents conditions experienced during heat waves, and ultimately drives the increased risk of kidney injury (via hyperthermia and/or dehydration) (5). However, ~160 min of whole body passive heating challenges the limit of subject tolerance. Alternative methods of obtaining serial sweat sample collections could be achieved pharmacologically. For example, previous work examining sweat rate and sweat composition in various skin types (e.g., tattooed vs. nontattooed skin) (39) has used pilocarpine, an acetylcholine agonist often used to promote sweating in clinical settings as a diagnostic test for cystic fibrosis (40). It should be noted, however, that there are methodological considerations when pharmacologically inducing sweating versus passive or exercise heat stress by resulting in differential sweat compositions (29). That said, the cross-body design in the present study would have ameliorated this methodological consideration and the purpose was not to assess sweat composition in the context of real-world settings.

A second consideration when utilizing passive heat stress in this model is that we were only able to obtain sweat samples at two timepoints (i.e., pre- and post-I/R). Therefore, the time course by which the sweat glands are impacted by I/R injury is unknown. For reference, Van Why et al. (13) observed a progressive decline in renal tubular reabsorption of sodium and reduction in Na^+-K^+-ATPase from 15 min following a reperfusion period (closest to the time course in the present study) and worst at 24 h.

Finally, relative to the magnitude and duration renal I/R injury in both a clinical context (e.g., cardiac bypass surgery, kidney transplantation) and during heat stress, the magnitude of I/R in the present study was likely lower. In rodent models, renal artery clamping to induce ischemia is ~60 min (9, 13) and upwards of hours in humans during surgery and potentially during heat waves. However, we selected the 20-min ischemia based on previous work from our laboratory (20) and others (17), which is sufficient in eliciting cutaneous microvascular dysfunction.

Conclusions

The present study provided the first evidence that sweat sodium concentration is elevated following I/R injury in humans. The data in the present study reveal that this elevation in sweat sodium concentration is likely not mediated by alterations in cutaneous microvascular function and/or active sweat glands, but may be contributed to by differential responses in local sweat rate following I/R. Further research is required to identify the mechanisms mediating altered sweat sodium reabsorption following I/R injury, which may include reductions in the active transport of sodium. Nevertheless, the present study established a model that future studies could leverage to understand the mechanisms of I/R injury-mediated impairments in tubular reabsorption of sodium during heat stress in humans. Such studies may have relevance for improving our understanding of the etiology of kidney injury during heat waves and further the understanding of how the kidneys and other tissues (e.g., eccrine sweat glands) reabsorb sodium.

DATA AVAILABILITY

Data will be made available upon reasonable request.

SUPPLEMENTAL DATA

Supplemental Table S1: https://doi.org/10.5281/zenodo.7709477.

ACKNOWLEDGMENTS

The authors thank the subjects for participating in our study. The authors also thank the Environmental Physiology Lab research technicians and other students for assistance during data collection. Graphical abstract and Fig. 1 created with BioRender and published with permission.

GRANTS

This work was supported by the National Institute for Occupational Safety and Health (R01OH011528; to Z.J.S.).

DISCLOSURES

This article's contents are solely the responsibility of the authors and do not necessarily represent the official views of the National Institute for Occupational Safety and Health. Z.J.S. has received consultant fees from Otsuka Holdings Co., Ltd. None of the other authors has any conflicts of interest, financial or otherwise, to disclose.

AUTHOR CONTRIBUTIONS

H.W.H., B.D.J., and Z.J.S. conceived and designed research; H.W.H., T.B.B., J.M.K., J.A.F., M.L.W., and Z.J.S. performed experiments; H.W.H. and Z.J.S. analyzed data; H.W.H. and Z.J.S. interpreted results of experiments; H.W.H. prepared figures; H.W.H. and Z.J.S. drafted manuscript; H.W.H., T.B.B., J.M.K., J.A.F., M.L.W., B.D.J., and Z.J.S. edited and revised manuscript; H.W.H., T.B.B., J.M.K., J.A.F., M.L.W., B.D.J., and Z.J.S. approved final version of manuscript.

REFERENCES

1. **Lim YH**, **So R**, **Lee C**, **Hong YC**, **Park M**, **Kim L**, **Yoon HJ.** Ambient temperature and hospital admissions for acute kidney injury: a time-series analysis. *Sci Total Environ* 616-617: 1134–1138, 2018. doi:10.1016/j.scitotenv.2017.10.207.
2. **Chapman CL**, **Johnson BD**, **Parker MD**, **Hostler D**, **Pryor RR**, **Schlader Z.** Kidney physiology and pathophysiology during heat stress and the modification by exercise, dehydration, heat acclimation and aging. *Temperature* 8: 108–159, 2021. doi:10.1080/23328940.2020.1826841.
3. **Miyamoto M.** Renal cortical and medullary tissue blood flow during experimental hyperthermia in dogs. *Jpn J Hyperthermic Oncol* 10: 78–89, 1994. doi:10.3191/thermalmedicine.10.78.
4. **Palmer LG**, **Schnermann J.** Integrated control of Na transport along the nephron. *Clin J Am Soc Nephrol* 10: 676–687, 2015. doi:10.2215/CJN.12391213.
5. **Hess HW**, **Stooks JJ**, **Baker TB**, **Chapman CL**, **Johnson BD**, **Pryor RR**, **Basile DP**, **Monroe JC**, **Hostler D**, **Schlader ZJ.** Kidney injury risk during prolonged exposure to current and projected wet bulb temperatures occurring during extreme heat events in healthy young men. *J Appl Physiol (1985)* 133: 27–40, 2022. doi:10.1152/japplphysiol.00601.2021.
6. **Levey AS**, **Eckardt KU**, **Dorman NM**, **Christiansen SL**, **Hoorn EJ**, **Ingelfinger JR**, **et al.** Nomenclature for kidney function and disease: report of a Kidney Disease: Improving Global Outcomes (KDIGO) Consensus Conference. *Kidney Int* 97: 1117–1129, 2020. doi:10.1016/j.kint.2020.02.010.
7. **Devarajan P.** Update on mechanisms of ischemic acute kidney injury. *J Am Soc Nephrol* 17: 1503–1520, 2006. doi:10.1681/ASN.2006010017.
8. **Schlader ZJ**, **Hostler D**, **Parker MD**, **Pryor RR**, **Lohr JW**, **Johnson BD**, **Chapman CL.** The potential for renal injury elicited by physical work in the heat. *Nutrients* 11: 2087, 2019. doi:10.3390/nu11092087.
9. **Wang Z**, **Rabb H**, **Haq M**, **Shull GE**, **Soleimani M.** A possible molecular basis of natriuresis during ischemic-reperfusion injury in the kidney. *J Am Soc Nephrol* 9: 605–613, 1998. doi:10.1681/ASN.V94605.
10. **Cooper JE**, **Wiseman AC.** Acute kidney injury in kidney transplantation. *Curr Opin Nephrol Hypertens* 22: 698–703, 2013. doi:10.1097/MNH.0b013e328365b388.
11. **Kwon O**, **Corrigan G**, **Myers BD**, **Sibley R**, **Scandling JD**, **Dafoe D**, **Alfrey E**, **Nelson WJ.** Sodium reabsorption and distribution of Na+/K+-ATPase during postischemic injury to the renal allograft. *Kidney Int* 55: 963–975, 1999. doi:10.1046/j.1523-1755.1999.055003963.x.
12. **Kwon TH**, **Frøkiaer J**, **Han JS**, **Knepper MA**, **Nielsen S.** Decreased abundance of major Na(+) transporters in kidneys of rats with ischemia-induced acute renal failure. *Am J Physiol Renal Physiol* 278: F925–F939, 2000. doi:10.1152/ajprenal.2000.278.6.F925.
13. **Van Why SK**, **Mann AS**, **Ardito T**, **Siegel NJ**, **Kashgarian M.** Expression and molecular regulation of Na(+)-K(+)-ATPase after renal ischemia. *Am J Physiol* 267: F75–85, 1994. doi:10.1152/ajprenal.1994.267.1.F75.
14. **Wilson TE.** Renal sympathetic nerve, blood flow, and epithelial transport responses to thermal stress. *Auton Neurosci* 204: 25–34, 2017. doi:10.1016/j.autneu.2016.12.007.
15. **Baker LB.** Physiology of sweat gland function: the roles of sweating and sweat composition in human health. *Temperature (Austin)* 6: 211–259, 2019. doi:10.1080/23328940.2019.1632145.
16. **Agu KA.** Can sweat glands act as temporary or permanent replacement for the excretory function of kidney. *Emer Life Sci Res* 3: 37–41, 2017. doi:10.7324/ELSR.2017.323741.
17. **McGarr GW**, **Hodges GJ**, **Mallette MM**, **Cheung SS.** Ischemia-reperfusion injury alters skin microvascular responses to local heating of the index finger. *Microvasc Res* 118: 12–19, 2018. doi:10.1016/j.mvr.2018.02.003.
18. **Bain AR**, **Jay O.** Does summer in a humid continental climate elicit an acclimatization of human thermoregulatory responses? *Eur J Appl Physiol* 111: 1197–1205, 2011. doi:10.1007/s00421-010-1743-9.
19. **Sawka MN**, **Burke LM**, **Eichner ER**, **Maughan RJ**, **Montain SJ**, **Stachenfeld NS**; **American College of Sports Medicine.** American College of Sports Medicine position stand. *Med Sci Sports Exerc* 39: 377–390, 2007. doi:10.1249/mss.0b013e31802ca597.
20. **Greenshields JT**, **Keeler JM**, **Freemas JA**, **Baker TB**, **Johnson BD**, **Carter SJ**, **Schlader ZJ.** Cutaneous microvascular vasodilatory consequences of acute consumption of a caffeinated soft drink sweetened with high-fructose corn syrup. *Physiol Rep* 9: e15074, 2021. doi:10.14814/phy2.15074.
21. **Byrne C**, **Lim CL.** The ingestible telemetric body core temperature sensor: a review of validity and exercise applications. *Br J Sports Med* 41: 126–133, 2007. doi:10.1136/bjsm.2006.026344.
22. **Hardy JD**, **Du Bois EF**, **Soderstrom GF.** The technique of measuring radiation and convection. *J Nutr* 15: 461–475, 1938. doi:10.1093/jn/15.5.461.
23. **Baker LB**, **Ungaro CT**, **Barnes KA**, **Nuccio RP**, **Reimel AJ**, **Stofan JR.** Validity and reliability of a field technique for sweat Na+ and K+ analysis during exercise in a hot-humid environment. *Physiol Rep* 2: e12007, 2014. doi:10.14814/phy2.12007.
24. **Gagnon D**, **Ganio MS**, **Lucas RA**, **Pearson J**, **Crandall CG**, **Kenny GP.** Modified iodine-paper technique for the standardized determination of sweat gland activation. *J Appl Physiol (1985)* 112: 1419–1425, 2012. doi:10.1152/japplphysiol.01508.2011.
25. **Chaseling GK**, **Crandall CG**, **Gagnon D.** Skin blood flow measurements during heat stress: technical and analytical considerations. *Am J Physiol Regul Integr Comp Physiol* 318: R57–R69, 2020. doi:10.1152/ajpregu.00177.2019.
26. **Tybout A**, **Sternthal B**, **Keppel G**, **Verducci J**, **Meyers-Levy J**, **Barnes J**, **Maxwell S**, **Allenby G**, **Gupta S**, **Steenkamp J-B.** Analysis of variance *J Consumer Psychol* 10: 5–35, 2001. doi:10.1207/S15327663JCP1001&2_03.
27. **Charkoudian N.** Skin blood flow in adult human thermoregulation: how it works, when it does not, and why. *Mayo Clin Proc* 78: 603–612, 2003. doi:10.4065/78.5.603.
28. **Johnson JM**, **Minson CT**, **Kellogg DL Jr.** Cutaneous vasodilator and vasoconstrictor mechanisms in temperature regulation. *Compr Physiol* 4: 33–89, 2014. doi:10.1002/cphy.c130015.
29. **Baker LB**, **Wolfe AS.** Physiological mechanisms determining eccrine sweat composition. *Eur J Appl Physiol* 120: 719–752, 2020. doi:10.1007/s00421-020-04323-7.
30. **Choi PJ**, **Brunt VE**, **Fujii N**, **Minson CT.** New approach to measure cutaneous microvascular function: an improved test of NO-mediated vasodilation by thermal hyperemia. *J Appl Physiol (1985)* 117: 277–283, 2014. doi:10.1152/japplphysiol.01397.2013.
31. **Minson CT.** Thermal provocation to evaluate microvascular reactivity in human skin. *J Appl Physiol (1985)* 109: 1239–1246, 2010. doi:10.1152/japplphysiol.00414.2010.
32. **Buono MJ**, **Claros R**, **Deboer T**, **Wong J.** Na+ secretion rate increases proportionally more than the Na^+ reabsorption rate with increases in sweat rate. *J Appl Physiol (1985)* 105: 1044–1048, 2008. doi:10.1152/japplphysiol.90503.2008.
33. **Wingo JE**, **Low DA**, **Keller DM**, **Brothers RM**, **Shibasaki M**, **Crandall CG.** Skin blood flow and local temperature independently modify sweat rate during passive heat stress in humans. *J Appl Physiol (1985)* 109: 1301–1306, 2010. doi:10.1152/japplphysiol.00646.2010.
34. **Sato K.** The physiology, pharmacology, and biochemistry of the eccrine sweat gland. *Rev Physiol Biochem Pharmacol* 79: 51–131, 1977. doi:10.1007/BFb0037089.
35. **Dobson RL**, **Sato K.** The secretion of salt and water by the eccrine sweat gland. *Arch Dermatol* 105: 366–370, 1972.
36. **Sato K**, **Dobson RL.** The effect of intracutaneous d-aldosterone and hydrocortisone on human eccrine sweat gland function. *J Invest Dermatol* 54: 450–462, 1970. doi:10.1111/1523-1747.ep12259279.
37. **Reddy MM**, **Quinton PM.** Functional interaction of CFTR and ENaC in sweat glands. *Pflugers Arch* 445: 499–503, 2003 [Erratum in *Pflugers Arch* 455:373, 2007]. doi:10.1007/s00424-002-0959-x.
38. **Goodman BE**, **Percy WH.** CFTR in cystic fibrosis and cholera: from membrane transport to clinical practice. *Adv Physiol Educ* 29: 75–82, 2005. doi:10.1152/advan.00035.2004.
39. **Luetkemeier MJ**, **Hanisko JM**, **Aho KM.** Skin tattoos alter sweat rate and Na+ concentration. *Med Sci Sports Exerc* 49: 1432–1436, 2017. doi:10.1249/MSS.0000000000001244.
40. **Webster HL.** Improved pilocarpine reservoir for use in sweat testing. *Clin Chem* 28: 2182–2183, 1982.